First results using PRIMA FSU as a fringe tracker for MIDI[*]

A. Müller[a,b], J.-U. Pott[b], S. Morel[c], R. Abuter[a], G. van Belle[a], R. van Boekel[b], L. Burtscher[b],
F. Delplancke[a], Th. Henning[b], W. Jaffe[d], Ch. Leinert[b], B. Lopez[e], A. Matter[e],
K. Meisenheimer[b], C. Schmid[a], K. Tristram[f], and A.P. Verhoeff[g]

[a]ESO, Karl-Schwarzschild-Str. 2, D-85748 Garching b. München, Germany
[b]Max-Planck-Institut für Astronomie, Königstuhl 17, D-69117 Heidelberg, Germany
[c]ESO, Casilla 19001, Vitacura, Santiago 19, Chile
[d]Sterrewacht Leiden, Leiden University, Niels-Bohr-Weg 2, 2300 CA Leiden, Netherlands
[e]Laboratoire Fizeau, UMR 6525, UNS - Observatoire de la Côte d'Azur, BP 4229, F-06304 Nice Cedex 4, France
[f]Max-Planck-Institut für Radioastronomie, Auf dem Hügel 69, D-53121 Bonn, Germany
[g]Astronomical Institute "Anton Pannekoek", University of Amsterdam, P.O. Box 94249, 1090 GE Amsterdam, The Netherlands

ABSTRACT

We report first results obtained from observations using a PRIMA FSU (Fringe Sensor Unit) as a fringe tracker for MIDI on the VLTI when operating with the 1.8-m ATs. Interferometric observations require the correction of the disturbance in the optical path induced by atmospheric turbulence ("piston"). The PRIMA FSU is able to compensate for such disturbances in real-time which makes it a suitable facility to stabilize the fringe signal for other VLTI instruments, like AMBER, MIDI or later MATISSE. Currently, the atmospheric coherence time in the N band (8 to 13 μm) observed by MIDI, as well as the thermal background in this band, require a minimum target flux of 20 Jy and a correlated flux of 10 Jy (in PRISM/HIGH_SENSE mode and using the ATs under standard conditions) to allow self-fringe-tracking and data reduction. However, we show that if the fringes are stabilized by the FSU, coherent integration allows a reliable data reduction even for the observation of faint targets ($F_{corr} <10$ Jy) with MIDI at standard detector exposure times. We were able to measure the correlated flux of a 0.5 Jy source, which pushes the current limits of MIDI down to regions where numerous new targets become accessible on ATs. For faint object observations we will discuss the usage of VISIR photometry for calibration purposes. The observational tests done so far and the obtained results represent a first step towards Phase Referenced Imaging with the VLTI in the mid-infrared.

Keywords: Interferometry, VLTI, MIDI, PRIMA, fringe tracking, high angular resolution, faint object observation

1. INTRODUCTION

MIDI (the mid-infrared interferometric instrument) on the Very Large Telescope interferometer (VLTI), is a two beam Michelson type interferometer producing dispersed fringes in the N band over a wavelength range from 8 to 13 μm.[1] A prism providing a resolution of R=30 and a grism providing a resolution of R=230 at λ=10.6 μm are the available dispersive elements. MIDI has two observation modes depending on two beam splitters in front of the beam combiner which reflect 30% of the incoming light into photometric beams which allows to measure the interferometric signal simultaneously to the photometric flux. This mode is called "science-photometry" (SCI_PHOT). If the beam splitters are not inserted, all incoming light is directly send to the beam combiner and is called "high-sense" mode (HIGH_SENSE). The most recent (as of ESO Period 86) official required minimum target flux for MIDI in HIGH_SENSE mode when observing with the 8-m unit telescopes (UT) or 1.8-m auxiliary telescopes (AT) are:

- **UTs:** Prism: $F_{tot}(12\mu m)$=1 Jy (N=4 mag), Grism: $F_{tot}(12\mu m)$=3 Jy (N=2.8 mag)

- **ATs:** Prism: $F_{tot}(12\mu m)$=20 Jy (N=0.75 mag), Grism: $F_{tot}(12\mu m)$=30 Jy (N=0.3 mag)

These limits arise from the atmospheric coherence time in the N band observed by MIDI, as well as the thermal background in this band and guarantee self-fringe-tracking and data reduction.

The mid-infrared wavelength range traces especially the dusty environment around stellar sources and makes MIDI suitable for the observation of a wide range of objects like active galactic nuclei (AGN), circumstellar and accretion disks around young stellar objects (YSO), and envelopes of Wolf-Rayet stars, Luminous Blue variable, B[e] supergiants, AGB stars, and post-AGB stars. In addition, the study of the mineralogy, composition, and the geometrical distribution of such dusty environments are possible using the N band. MIDI is extensively used since it was offered in 2004, resulting in more than 80 refereed journal articles so far, making it the world's most prolific interferometric instrument to date.

In 2008 the installation and commissioning of the PRIMA[2,3] (phase-referenced imaging and micro-arcsecond astrometry) dual-feed facility at VLTI started and is still ongoing.[4] Once fully operational, PRIMA will be used for faint-object observations, phase-referenced imaging using AMBER and MIDI, and narrow-angle astrometry.[3] PRIMA comes with four sub-systems: the fringe sensor unit (FSU), the star-separator module (STS), differential delay lines (DDL), and the internal laser metrology. The PRIMA FSU consist of two identical interferometers (FSU-A and FSU-B) working in K band. For a detailed description of the FSU and its current performance we refer to Ref. 5 and 6. Their design and sensitivity allow to estimate of phase delay and group delay in real time in order to correct for atmospheric turbulence effects ("piston") which causes random variations of the optical path difference (OPD). The operation and sensitivity in the K band makes the FSU an especially suitable fringe tracker for MIDI compared to FINITO[7] which is an H band fringe tracker at VLTI. FINITO has a point source sensitivity of H=5 mag on ATs which typically delivers enough photons in N for standard MIDI self-fringe-tracking operation. In addition, many sources such as YSOs are very red sources and therefore faint in the H band. Also, the problem of MIDI+FINITO is the usually over-resolved diameter in H band compared to N band. Using PRIMA FSU with MIDI alleviates this problem.

In the following sections we will present first results of observations using MIDI+FSU in on-axis mode and its promising capabilities for various science cases. If not otherwise indicated the expression MIDI+PRIMA in the following sections refers to MIDI observations using PRIMA FSU-A as a fringe tracker in single-feed, on-axis mode.

2. OBSERVATIONS AND DATA REDUCTION

2.1 VLTI and Instrument Setup

Two of the VLTI's four 1.8-m auxiliary telescopes send the light to the main delay lines; for the results herein, these were AT1 and AT2. The M12 mirrors send the light beams into the lab where they pass the switchyard which brings it on the designated beam paths. A dichroic mirror in the light path sends the N band to MIDI while the near infrared part of the light passes the dichroic mirror. Another dichroic mirror on the PRIMA bench send the H band to the IRIS[8] tip-tilt corrector while the K band goes to FSU-A.

For the MIDI+PRIMA single-feed mode there were no additional hardware modifications of the VLTI lab necessary in order to send the light to each instrument. The co-alignment of the FSU-A on MIDI could be easily achieved by applying an offset of 300 μm using a translation stage of FSU-A in order to correct for the difference in OPD between both instruments. MIDI in standard operation provides internal fringe tracking on the basis of group delay fringe tracking and therefore sends correction to the VLTI delay lines. In order to use FSU-A as a fringe tracker, the `minrts` module (the MIDI Near Real Time System[9]) had to be modified. In addition, the MIDI observation template was modified to set FSU-A as the fringe tracker.

2.2 Demonstration Observations

Observations were carried out during PRIMA commissioning runs (hereafter COM) 6, 8, and 9 on a back-up basis without impacting the higher priority astrometric commissioning tasks. Tab. 1 gives an overview of all observations. The observed stars are mainly MIDI calibrator stars with known fluxes and apparent diameters and were observed to characterize the MIDI+PRIMA single-feed, on-axis mode. In all cases, FSU-A was operated at 1kHz.

Run	Date	Telescope	Station	BL [m]	n_{stars}	$F_{tot,12\mu m}$ [Jy]	P/G	n_{frames}
(1)	(2)	(3)	(4)	(5)	(6)	(7)	(8)	(9)
COM6	2009 Jul. 25	AT1-AT2	D0-A0	32	9	6.6 – 163.0	Prism	8000
COM8	2009 Oct. 11	AT1-AT2	D0-A0	32	7	1.0 – 8.6	Prism	8000
COM9	2009 Dec. 10-12	AT1-AT2	H0-D0	64	22	0.47 – 56.8	Prism/Grism	16000

Table 1. Overview of all MIDI+PRIMA single-feed test observations carried out so far. The columns are (1) COM ID and (2) the date when the observations took place; (3) used telescopes and (4) the used VLTI stations; (5) baseline; (6) total number of observed stars; (7) the range of total fluxes at 12 μm; (8) used dispersive element of MIDI; (9) the total number of recorded MIDI frames per observation.

2.3 Data Reduction

The data reduction was performed with EWS (Expert Work Station[†], Version 2009Dec02), a data reduction package based on the coherent data reduction method. A detailed description of EWS is found in Ref. 10.

The format of the timestamps differ between MIDI and FSU-A. The MIDI frames are recorded using the modified Julian date (MJD) as timestamp while the FSU-A timestamps are in microseconds. In addition, a typical exposure of MIDI (Prism/HIGH_SENSE) takes 20ms compared to 1ms for FSU-A, i.e. during one MIDI exposure around 20 FSU-A frames were recorded. Additional routines to the EWS pipeline have been written using the `Octave` numerical computation language and then the Interactive data language (IDL) in order to match the FSU-A frames to the corresponding MIDI frame. Different reduction strategies were used:

- Method 1: standard EWS reduction (MIDI group delay is used, FSU-A data are not considered at all, for a detailed description of the reduction steps we refer to Ref. 10)

- Method 2: "quasi-coherent" reduction (MIDI is coadding the fringes directly as provided by FSU-A fringe tracking)

- Method 3: standard EWS reduction but using the group delay measured by FSU-A in the *K* band to derotate the MIDI fringes

The selection of MIDI frames of the latter two methods is based on the fringe tracking performance of the FSU-A, i.e.

- FSU-A has to track on the fringe during one MIDI exposure (20ms), this selection is based on the state of the OPD controller (OPDC, see Ref. 5)

- the FSU-A group delay residuals need to be lower than a certain threshold during one MIDI exposure

The results of the different reduction strategies are presented in Sec. 3.

3. RESULTS

3.1 Stabilizing the Fringe Signal

Fig. 1 shows a part of the MIDI real time display visible during observations. Each vertical line corresponds to the average Fourier transform of the frames of the same scan of the channeled spectrum and the horizontal axis of the plot can be interpreted as a time axis. Therefore, one can follow by eye the change in OPD (and therefore of the change in group delay, too) with time. Fig. 1a shows the signal of a typical observation when MIDI is operated without an external fringe tracker. The scatter in time caused by the atmospheric piston turbulence is clearly visible. The situation changes dramatically when FSU-A as a fringe tracker is used and the fringe signal gets stabilized by FSU-A (see Fig. 1b) where a more substantial portion of the atmospheric piston turbulence get corrected. Typical group delay residuals for MIDI "alone" are ≈30–35 μm. Using FSU-A as a fringe tracker the group delay residuals in *N* band can go down to 1.5 μm.

To reduce the MIDI data with the different reduction strategies listed in Sec. 2.3 it is necessary, amongst others, that

---

[†]The software package "MIA+EWS" is available for download at
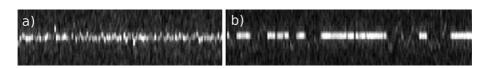`http://www.strw.leidenuniv.nl/~nevec/MIDI/index.html`

Figure 1. Snapshot of the MIDI real time display visible during observation showing the average Fourier transform of the frames of the same scan of the channeled spectrum for MIDI without (a) and with (b) fringe tracker. The gaps visible in the right plot (b) are periods where FSU-A lost the fringe.

the group delay measured by both instruments in the K and N band are correlated, e.g., in order to be able to derotate the MIDI fringes with the K band group delay (Method 3). This applies especially for objects with too faint correlated N band fluxes where a measurement of the N band group delay is no longer possible. An example of the behavior of both group delays is shown in Fig. 2. It is an observation of the bright star HD186791 ($F_{\text{tot}}(12\mu m) = 76$ Jy). The upper left plot shows the MIDI group delay, the middle left plot shows the FSU-A group delay. The values are plotted over the already from the reduction process selected "good" frames (see Sec. 2.3). The FSU-A group delay values are the mean values of the single FSU-A frames which belong to one single MIDI frame. The lower left plot shows the cross correlation function between both group delay values. Both group delay values are plotted to each other in the plot on the right side. The red line is a linear fit with slope one. The strong correlation between the K and N band group delay values is evident.
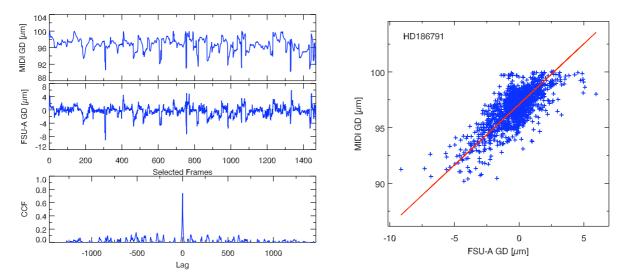

Figure 2. Upper left: MIDI group delay of selected "good" frames and the K band group delay measured by FSU-A displayed in the middle left plot. Lower left: cross correlation function between both group delay values. Right plot: MIDI group delay vs. FSU-A group delay. The red line is a linear fit with slope one.

3.2 Correlated Flux

Examples of the correlated fluxes determined by the different reduction strategies presented in Sec. 2.3 are shown in Fig. 3. Each plot belongs to a single observation and shows the measured uncalibrated correlated flux over the N band. The green line belongs to reduction method 1 (standard EWS), the red line belongs to method 2 ("quasi-coherent"), and the blue line belongs to the 3rd method (using FSU-A group delay instead of the N band group delay). It is clearly visible that the reduction methods 2 and 3, which are based on the FSU-A fringe tracking performance, deliver at least as high raw correlated fluxes as the standard EWS reduction process. The reason for the slightly lower raw correlated flux obtained by EWS might be due to the lower accuracy to which the N band group delay can be measured compared to the group delay measured by the FSU-A in K band. This is an important fact concerning the reduction of faint object observations where the signal is too faint in order to measure a group delay in N band (see Sec. 3.3). In addition, since FSU-A stabilizes the fringes to better than $\lambda/10$ for the N band, method 2 is sufficient in most cases.
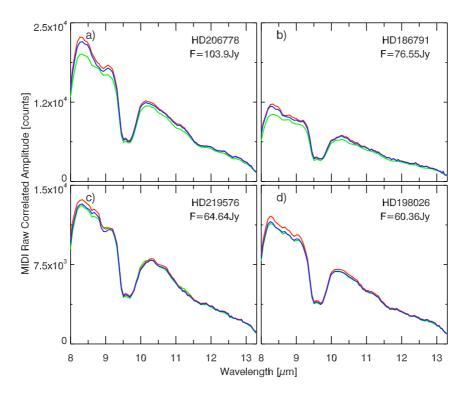
Figure 3. Measured raw correlated fluxes of four stars. Green line: standard EWS (method 1), red line: "quasi-coherent" integration (method 2), blue line: standard EWS but instead of derotating the fringe signal with N band group delay, the FSU-A group delay (K band) was used (method 3).

3.3 Faint Object Observations

For the flux limits listed in Sec. 1 photometry (F_{tot}) taken by MIDI of sufficient quality can be guaranteed. The limit for correlated flux observations is lower by a factor of two. To calculate the visibility $V=F_{corr}/F_{tot}$ both values are needed. However, we were able to measure the faintest correlated fluxes of stars ever observed at the ATs using PRIMA FSU-A as an on-axis fringe tracker for MIDI. With the prism we observed HD56470 with $F_{tot}(12\mu m)$=0.47 Jy which is equivalent to N=4.8 mag (see left plot of Fig. 4). Using the grism, we could measure a correlated flux for the $F_{tot}(12\mu m)$=2.2 Jy (N=3.1 mag) source HD46308 (see right plot of Fig. 4). We used for both stars the "quasi-coherent" data reduction method (method 2, see Sec. 2.3), because the fringe signal in the N band got sufficiently stabilized by the fringe tracker. This achieved sensitivity of MIDI when PRIMA FSU is used as a fringe tracker is a clear demonstration of one of the new capabilities of this mode. Therefore, it is possible with the ATs to observe most of the targets that were previously only accessible by the UTs, which have 20 times the collecting area. The advantages of the usage of the ATs are obvious:

- the ATs are dedicated to pure interferometric observations

- it can reduce the overbooking pressure on the UTs, i.e. more observations (interferometric and non-interferometric) are possible

- due to the 30 dedicated stations for the ATs, dozens of baselines ranging from 8 m to 200 m at different position angles are available, though not all of them at the same time (for comparison: the four UTs can only provide six fixed baselines ranging from 46 m to 130 m)

The left plot of Fig. 5 shows the over the wavelength range of 10 to 10.5 μm averaged raw correlated flux (measured with the "quasi-coherent" method) of all observations with MIDI using the prism plotted over the total flux at 12 μm measured by IRAS.[11] The gray dashed line is a linear fit to the data. A linear relation is only expected under the assumption of
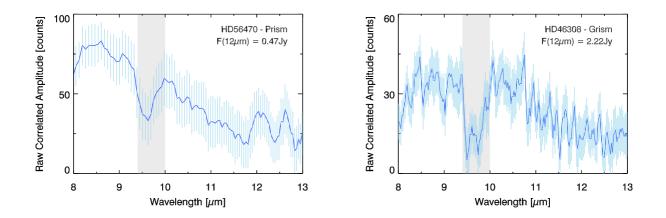
Figure 4. Left: Raw correlated flux of star HD56470 ($F_{tot}(12\mu m)$=0.47 Jy) observed during COM9 with the ATs and with MIDI in Prism/HIGH_SENSE mode. Right: Raw correlated flux of star HD46308 ($F_{tot}(12\mu m)$=2.2 Jy) observed during COM9 with the ATs and with MIDI in Grism/HIGH_SENSE mode. The strong ozone absorption feature is clearly visible in both plots and marked by the vertical gray region.

unresolved sources, i.e. that the correlated flux is equal to the total flux. If the lower sensitivity limit would have been reached, the correlated fluxes would be constant at a certain point and only the residuals of the sky background substraction from the N band would be visible. Because this seems to be not the case for the data available, a lower limit of around 0.5 Jy for the correlated flux detectable seems to be reasonable. The right plot of Fig. 5 shows the corresponding relative errors of the measured correlated fluxes. An increase of the relative errors with decreasing correlated flux is clearly visible and indicates a lower limit of around 0.5 Jy for the correlated flux, too.
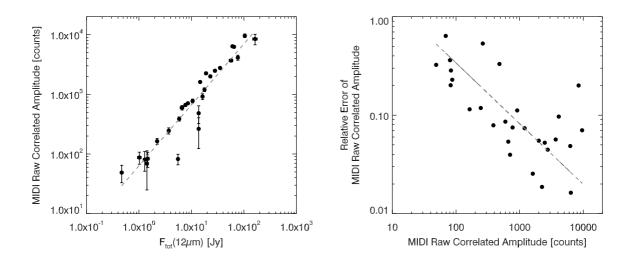

Figure 5. Left: Averaged (over the wavelengthrange of 10 to 10.5 μm) raw correlated flux of all prism data that were obtained with the MIDI+FSU-A on-axis mode. Right: Corresponding relative errors of the measured correlated fluxes. The trend in both plots indicate a limit of around 0.5 Jy of correlated flux which can be observed by MIDI with FSU-A as a fringe tracker for the ATs.

3.4 Calibration of the Data

The raw correlated flux can vary during an observation caused by an insufficient tip-tilt and piston correction of the fringe tracker or other subsystems. This leads to an decrease of the measured correlated flux because of the averaging of the

values of each frame. In order to visualize this effect we binned one MIDI observation of the star HD198026 where 8000 frames were recorded into 16 bins containing 500 successive frames. Each bin was handled as a single observation, i.e. was reduced independent from the other bins. The upper left plot of Fig. 6 shows the measured raw correlated flux of each bin. The small numbers inside the plot indicate the total number of used MIDI frames of each bin based on the FSU-A fringe tracking performance. As expected, the correlated flux varies during the observation ranging from 5500 to 7000 counts in this example. In the lower left plot of Fig. 6 the computed K band residual group delay values of FSU-A are plotted for each bin. A comparison by eye already reveals a correlation. For bins with higher group delay residuals the measured correlated flux is lower as well as the used number of MIDI frames in this bin. Plotting the N band correlated flux over the FSU-A group delay residuals (plot on the right side of Fig. 6) shows this effect clearly. The theoretical correlated flux $F_{corr,0}$ that can be measured is decreased by a factor depending on the value of the residual group delay σ_{GD}, see Eqn. 1.

$$F_{corr} = F_{corr,0} \exp\left[-2 \cdot \left(\frac{\pi \cdot \sigma_{GD}}{\lambda} \right)^2 \right], \qquad (1)$$

where F_{corr} is the measured correlated flux and λ is the wavelength considered. The red line in this plot represents a fit using Eqn. 1 and describes the measured values quite well. This relation could now be used to correct the raw correlated flux measured by MIDI to zero FSU-A group delay frame-wise, i.e. to the theoretical case that the fringe tracker worked perfectly and corrected for all distortions occurred during the observation. This would lead to a greater and - more importantly - a much more accurate determination of the correlated flux. Deviations from this correlation might come from bad beam-overlap, low SNR in a certain bin, etc., which would explain the outlier points in the right plot of Fig. 6.
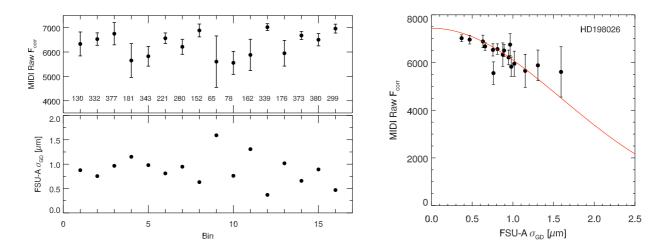

Figure 6. MIDI+FSU-A observation of HD198026 with 8000 recorded MIDI frames. The observation was binned into 500 frames wide bins and separately reduced. Upper left: N band raw correlated flux measured in each bin and the corresponding K band residual group delay computed from the FSU-A data (lower left plot). On the right side both quantities are plotted against each other. The red line represents a fit to the data using Eqn. 1. See text for explanation.

To obtain calibrated MIDI data, i.e. correlated flux in Jy and calibrated visibilities, depends on the source photometry taken by MIDI in case of the standard observation. Correlated flux measurements can always be calibrated without having photometry of the science target available (see Ref. 12 for a detailed explanation) independent if the source is a bright or faint one. Having measurements of the correlated flux with a sufficient number of baselines and position angles, a physical interpretation of the object is already possible without having calibrated visibilities (demonstrated by, e.g. Ref. 13). With MIDI a calibrated visibility is obtained by dividing the calibrated correlated flux by the calibrated total flux of the science object, $V = F_{corr}/F_{tot}$. Observing sources with $F_{tot} < 20$ Jy with the ATs, a proper photometry can no longer be extracted. However, there exist the possibility to obtain N band photometry from, e.g. VISIR at VLT or from the infrared satellite Spitzer. But there are several constraints in order to be able to use the photometry from these instruments to calibrate MIDI visibilities:

- The science object cannot be more extended in the *N* band than the slit width of the used instrument. Otherwise the visibilities get overestimated. Typical slit with of VISIR is 0.75 arcsec and 3.6 arcsec for Spitzer on sky. The 200 μm slit of MIDI corresponds to 2.3 arcsec on sky using the ATs.

- The MIDI observations and the Spitzer/VISIR need to be sufficiently close in time, such that any possible object variability in the *N* band is small compared to the measurement error in correlated flux. In principle it is possible to take a VISIR spectrum in parallel to MIDI+PRIMA observations (with ATs) if needed for time variability.

For the Herbig Ae/Be star HD135344B we demonstrated exemplarily the possibility to get calibrated visibilities by taking the photometric levels from a VISIR spectrum. The MIDI observations were carried out using the UTs in June 2006 and are originally published in Ref. 14. Fig. 7 shows the calibrated visibility data (blue points) obtained from the standard reduction process, i.e. calibration of the visibility using source photometry taken with MIDI. The dataset was again reduced but this time the MIDI photometry of the science source was not considered at all. A spectrum from VISIR[15] taken in July 2007 was then used to compute a second set of calibrated visibilities (red points). Because the source did not show any variability in the period between the MIDI and VISIR measurements and its apparent size on sky is smaller than the used slit width of VISIR, the visibility values are quantitatively and qualitatively similar to the values obtained with MIDI alone. In addition, VISIR delivers a much more accurate photometry compared to MIDI resulting in much smoother visibility curve with smaller error bars.
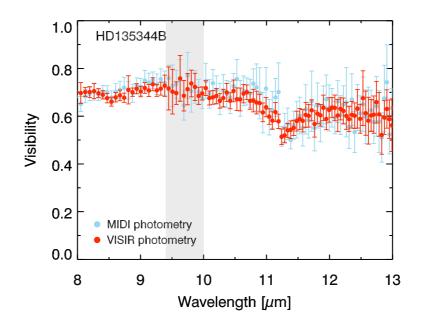

Figure 7. Calibrated visibilities of the young Herbig Ae/Be star HD135344B. The blue points are the visibilities obtained by using MIDI photometry. A re-reduction of the MIDI data but using VISIR photometry instead, delivers the same visibilities (red points). In both cases, the observed calibrator star HD129456 was used in order to take the interferometric transfer function into account. The vertical gray region is characterized by the strong ozone absorption band. Residuals of the data reduction may be present within these region.

In order to stress out the usage of external photometry under certain circumstances and its constraints, we summarize important points in the following.

- difficulties with photometry by MIDI occur for very faint sources only

- for faint sources where no photometry can be obtained by MIDI but a correlated flux can be measured using MIDI+PRIMA there will be at least an interferometric measurement/information available at all

- for these sources, accuracies better than 10% cannot be expected

- some scientific questions (e.g. comparison of different position angles) can be done on the basis of correlated fluxes without photometry

- the field of view of VISIR of 0.56 arcsec at 10 μm is very similar to the MIDI slit width of 0.52 arcsec at the UTs

- the spectral resolution of VISIR with respect to MIDI can be made more similar by smoothing VISIR data

- the observation of the - usually bright - calibrator with VISIR and MIDI allows transformation directly into the MIDI system

- VISIR observations should be possible within one week of the MIDI observations, if not better

- the variability of AGNs may be slower than that

- the variability of T Tauri stars is much stronger at short wavelengths (U, B, V), at H and K already not large compared to 10% even over longer periods than one week, at 10 μm hopefully probably less

4. SCIENCE CASES

In this section we list science cases that can only be carried out using PRIMA FSU as a fringe tacker for MIDI as well as some explicit numbers of doable objects of such an operating mode.

4.1 The Structure of Active Galactic Nuclei

The current interesting problem of AGNs is that in every AGN that we studied with more than just a few baselines we see that simple geometrical models do not work very well (e.g. Circinus,[13] NGC1068,[16] Cen A[17]). This might indicate "clumpiness" of the torus. Since hydrodynamical models do not yet predict specific clumpy patterns for individual sources that we could test with our observations, we need observational input to find out which clumpy patterns could explain the visibilities that we observe. This is not just a matter of time but of {u,v} plane coverage.

Single-Feed, On-Axis   With the current assumption of a limiting magnitude of $K \approx 8$ mag with the ATs for PRIMA FSU there are four sources (NGC1068, Circinus, NGC4151, RX J1029.1+2729) that are worth trying with the on-axis strategy. These sources have all succesfully been observed with MIDI and we estimate the observations of new sources will only become possible once $K \approx 11$ mag is reached (i.e. an appealing opportunity for MIDI+PRIMA with the UTs).

Dual-Feed, Off-Axis   What is much more interesting is the use of off-axis tracking (dual-feed). Circinus has a K=7.5 mag star 53 arcsec away from the nucleus, Centaurus-A has a K=9.1 mag star 44 arcsec away. With these we might not need any UT observations for these sources any more while being able to drastically increase the UV coverage using all available AT baselines. This is extremely interesting as both sources seem to have rather complex structures so that a good sampling of the visibility/correlated fluxes is very important. There are two more sources with a reference star with K<10 mag: Mrk1095 and LEDA59124. Both have also been observed with MIDI before, so F_{corr} >0.1 Jy. The next interesting source is 2E 0507.8+1626 with an N band flux of 0.4 Jy and a K=6.2 mag star at a distance of 32 arcsec. A cross correlation between the Véron-Cetty AGN catalogue (DEC<40°, z <0.5, V<20 mag) and the 2MASS catalogue gives 56 AGN with a K<8 mag nucleus or a K<8 mag star within 55 arcsec. Only 12 of the AGN are actually "nearby", i.e. with z <0.05. One interesting aspect when using an offset reference star, is the possibility to at the same time with FSU-A measure the NIR correlated flux and phase of the AGN and see whether we can detect an offset between the NIR and the MIR source.

4.2 GCIRS7 - the Bright Supergiant at the Galactic Center

A technically challenging science case is provided by GCIRS7, the bright supergiant at the Galactic center, merely 5 arcsec away from the supermassive black hole SgrA*. As shown in previous MIDI observations,[18] the circumstellar matter is resolved with the VLTI and probably related to a shock front. Studying the detailed geometry of this shock front with the increased uv-coverage and phase information of MIDI+FSU would help to distinguish between a collision with stellar winds from the nearby IRS16 cluster, or in contrast with a possible outflow of SgrA* itself.

Furthermore, if the FSU can track AT-fringes on GCIRS7, and the star separators become available, a suite of unique Galactic center science cases will become accessible.[18]

4.3 Direct detection of extrasolar giant planets with MIDI and PRIMA

Required accuracy on the differential phase measurement for close-in extrasolar planets Differential interferometry represents an innovative direct detection method that may allow observers to obtain spectroscopic information, planetary mass, and orbit inclination of extrasolar planets around nearby stars using the current ground-based long-baseline interferometers, such as the VLTI (see Ref. 19 and 20) or the Keck Interferometer (see Ref. 21). Detection and characterization of close-in extrasolar giant planets (EGPs) may be foreseen with the MIDI instrument by using differential phase (see Ref. 22). Our considered exoplanet named Gliese 86b[23] presents a flux ratio with its parent star, Gliese 86, much more favorable in N band ($\approx 10^{-3}$) than in the NIR ($\approx 10^{-5}$) or the visible ($\approx 10^{-6}$) (see Fig. 8). In N band, the expected differential phase signal produced by the planet is quite linear and has a typical amplitude of about 0.1 deg (see Fig. 8). However, instrumental and atmospheric stability introduce some limitations. In N band, two contributions can strongly affect the interferometric measurements:

1. The overwhelming sky background emission, which can generally be removed by subtracting the two π-phase-shifted interferometric channels of MIDI. In terms of fundamental noise, regarding the SNR estimations on the differential phase (see Ref. 24), at least 5 hours of observation with the UTs would be required to allow a 3σ detection of Gliese 86b in N band.

2. The strong chromatic dispersion due to the water vapor (see Ref. 25 and Ref. 26), which appears very limiting and difficult to calibrate. Nevertheless the strong chromatic dependence of the flux ratio between the planet and the star, could help in that case, as described below.
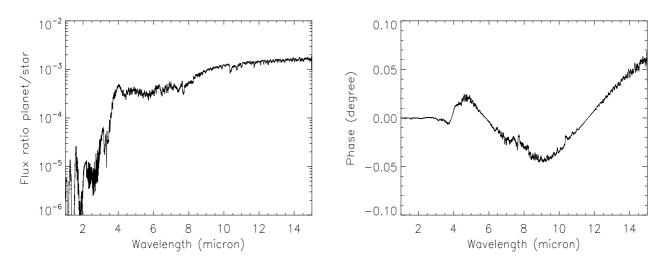

Figure 8. Left panel: Expected flux ratio between Gliese 86b and its star between 1 and 15 μm. Right panel: Theoretical interferometric phase of the GL86 system between 1 and 15 μm; the projected baseline used here is equal to 110 m for a baseline value of 130 m at ground level. For these two figures, which have been smoothed for sake of clarity, the planetary radius is assumed to be 1.2R$_{\text{jupiter}}$.

Limiting factor: water vapor fluctuations The dispersive contribution due to water vapor and affecting the phase measurement in N band can be written under the following form :

$$\Phi_{\text{disp}}(\lambda, t) = \frac{2\pi}{\lambda} OPD_{\text{wv}}(\lambda, t) \tag{2}$$

The OPD term contains a dominant achromatic term corresponding to the uncorrected achromatic delay (or "piston") between beams, and a chromatic term representing the higher order dispersion. A linear fit on the phase is usually performed to estimate and remove the achromatic term affecting the measured differential phase. Unfortunately, this operation also removes any linear trend due to the planet signal.

After such correction, the phase is constituted by the non-linear contribution of the dispersion along with the remaining planet signal, both having a curvature-like or quadratic aspect. The amplitude of the curvature introduced by the non-linear dispersion term can typically reach at least a few degrees (see Ref. 27) and overwhelm the curvature due to the planet which now has an amplitude of about 0.03 deg as shown in Fig. 9.
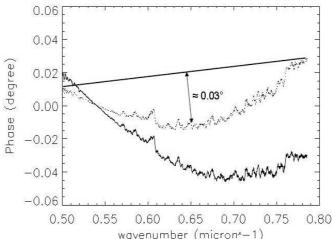

Figure 9. Illustration of the expected amplitude of the planet signal as a function of wavenumber (k) in N band. In this example, we consider a projected baseline of 110m, and a planetary radius of $1.2R_{\mathrm{jupiter}}$. The solid line curve corresponds to the total theoretical phase, while the dotted line one corresponds to the theoretical phase after fitting out the linear part (called 'de-pistoned' phase). The vertical arrow represents the approximative expected amplitude of that de-pistoned phase.

Calibration of water vapor dispersion effects For the sake of detection, an additional correction is thus required. For that it is convenient to make the remaining chromatic part of OPD_{wv} explicit as a function of one single achromatic parameter, $f_{\mathrm{wv}}(t)$, containing all the contributions that affects the dispersion amplitude:

$$\Phi_{\mathrm{disp}}(\lambda, t) = \frac{2\pi}{\lambda} \cdot R_{\mathrm{wv}}(\lambda) \cdot f_{\mathrm{wv}}(t) \tag{3}$$

Here $R_{\mathrm{wv}}(\lambda)$ is the known specific refractivity of water vapor, calculated from the various absorption resonances of this constituent. As shown in Fig. 8, the flux ratio, hence the interferometric phase signal of Gliese 86b, is negligible in the NIR (1 to 2.5 μm) (see Fig. 8). Therefore to measure and correct the water vapor dispersion, one solution is to estimate the amplitude of the water vapor dispersion, that is $f_{\mathrm{wv}}(t)$, using the differential phases measured in K band. Then, the dispersion parameter could be applied to the phases simultaneously obtained in N band and containing the remaining planet signal. This approach would allow a N band chromatic water vapor modelling and correction, which would preserve the planetary signal.

Current results obtained with MIDI+AMBER Performed in November 2007 as a part of the MIDI Guaranteed Time Observation Exoplanet Programme, the observation of Gliese 86b constituted the first attempt at an exoplanet detection with MIDI. It is also a technical achievement since it motivated the first VLTI observation using AMBER and MIDI simultaneously. For the first time, the instruments MIDI (8-13 μm) and AMBER (1-2.4 μm) were simultaneously used for the observation of Gliese 86. In principle, this implies that the two instruments have similar transversal alignment, longitudinal alignment, and temporal synchronicity. In practice, each of these adjustments has only been approximated, as best as possible. This resulted in a significant degradation of both MIDI and AMBER data, preventing a direct application of the calibration method described above. Nevertheless, a feasibility study was performed from the data of our MIDI GTO observations of November 2007.

Based on the MIDI phase measurements of the calibrator HD9362 (the Gliese 86b data being unusable), our study showed that a precision on the curvature measurement of about 0.33 deg is currently reached. Consequently, the current detection

limit is a factor 10 above the precision required to achieve the planet phase signal in *N* band.

In terms of accuracy of calibration of the water vapor dispersion, using the AMBER data obtained in *K* band, we can infer that we approximately stand at a factor of 10 above the phase signature from the planet.

As a conclusion, it appears that we are currently limited at the same level regarding the curvature measurement in *N* band, and the calibration of the water vapor dispersion using the *K* band data. These results are extensively described in Ref. 28.

Application to the PRIMA on-axis observing mode In the framework of the exoplanet direct detection by interferometry, this first attempt constitutes a strong motivation for the simultaneous use of the spectroscopic mode of PRIMA with MIDI. In on-axis fringe tracking mode, PRIMA could be used to measure the *K* band amplitude of the water vapor dispersion by the intermediate of its spectroscopic mode (five spectral channels). Moreover, since PRIMA has been designed to operate simultaneously with other scientific instruments like MIDI, the parallel operation can be done under the best conditions. A much better quality and calibration accuracy of the MIDI data are thus expected. In terms of thermal background noise and flux level of the source, a future observation of Gliese 86b with PRIMA and MIDI would require in addition the use of UTs, an observing time of about 10 hours including the source and the calibration stars, and no chopping procedure. In terms of perspective, this project of direct detection by differential interferometry with PRIMA and MIDI could be extended to about eight other exoplanets (see Ref. 24). This science case is an outlook once we know what our limits on the differential phase are.

4.4 Young Stellar Objects

MIDI with FINITO[7] has been almost never used for scientific observations, simply because the point source sensitivity of *H*=5 mag on ATs was inferior to what MIDI could achieve by self-fringe tracking. In addition, YSOs are very red sources and therefore faint in the *H* band. Also, the problem of MIDI+FINITO is the usually over-resolved diameter in *H* band compared to *N* band. We will demonstrate that the situation using PRIMA FSU-A as on-axis fringe tracker for MIDI is completely different, and very promising. This observing mode is expected to be somewhat more sensitive than dual-beam off-axis fringe tracking, which is important in particular for the young stars programme.

It is assumed that the point source limiting magnitudes for on-axis fringe tracking with MIDI, using PRIMA FSU-A as fringe tracker, are *K*=8.0 mag on ATs and *K*=10 mag on UTs. Perhaps it will turn out that these even are conservative estimates. For most of such sources acquisition and guiding using adaptive optics and/or tip-tilt correction should be possible.

Expected gains for observations with MIDI The basis for the gains is the higher sensitivity, much improved with respect to FINITO. We discuss the different gain aspects separately although they are of course related.

Gain by increased number of sources This gain is particularly evident for young star sources. Fig. 10 shows the *K* band brightnesses of young low mass stars in two well-studied nearby star forming regions. For a sensitivity limit of *H*=5 mag, corresponding in average to *K*=4.3 mag, no single one of these objects is doable (Z CMa is an exception, being a FU Ori/Herbig Ae/Be star binary). However, with the limiting magnitudes around *K*=8 mag expected with PRIMA, a sizeable fraction, dozens of objects, come into reach for the ATs, and on the UTs the number of doable sources gets about doubled. For Herbig Ae/Be stars (young intermediate mass stars) and candidates, out of 245 possible sources, right now about a twenty can be done on ATs (see plot on the right side of Fig. 11). With PRIMA, this number would rise to ≈130 sources with *K*<8 mag (see left plot of Fig. 11) and $F_{corr}(12\mu m)$<10 Jy which would be accessible with the ATs.

For high-mass young stars, the gain in the number of doable sources is less pronounced but still an important increase. With the larger number of observable sources it will become possible to do dedicated studies on groups selected by physical criteria, simply because the largely increased number of sources now allows a selection.

Gain by improved sensitivity The increased sensitivity expected with PRIMA in general increases the number of observable sources but specifically also gives access to individual particularly interesting sources which are too faint to be routinely observed with the VLTI, even on UTs. An example is TW Hya, the most nearby classical T Tauri star where the disk structure of such sources can best be studied. With *V*=11.1 mag, *H*=7.6 mag, *K*=7.3 mag, *N* band flux 0.2-0.8 Jy it is barely doable on UTs under excellent conditions - attempted additional observations under normal conditions failed so
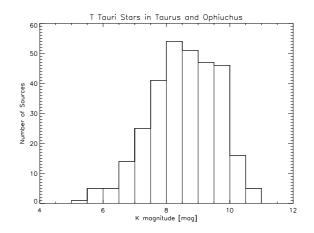
Figure 10. *K* band brightness distribution of young low mass stars in the Taurus and Ophiuchus star forming regions.
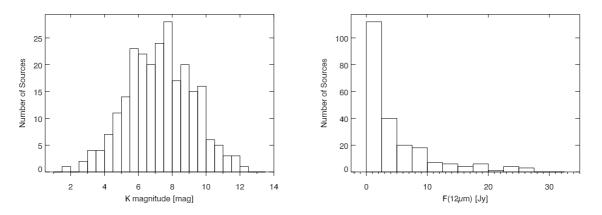

Figure 11. *K* band brightness (left) and MIR flux distribution of young Herbig Ae/Be stars and candidates.

far. With PRIMA on axis fringe tracking, this source should be well observable even on ATs, allowing the desired detailed studies.

Gain in technical aspects   With PRIMA fringe tracking many fainter sources will become accessible on the ATs especially due to the gain in sensitivity of MIDI. This has the scientific advantage, that a larger number of baselines, and in particular short baselines (8-30 m), will be available in principle. The latter is an important aspect for most programmes performed with MIDI.

4.5 Other Objects

Many of the hot stars surrounded by circumstellar matter have very low visibilities, leading even for bright sources to low correlated flux. With PRIMA, these sources also will be open to study. Examples of hot sources with dusty environments: Wolf-Rayet stars, Luminous Blue variable, and B[e] supergiants, large cold supergiants with dense circumstellar material (AGBs, post-AGBs).

5. CONCLUSIONS AND OUTLOOK

The data in this article demonstrate that the VLTI and PRIMA infrastructure and hardware, as available, allow to run MIDI+PRIMA on-axis in parallel with the benefit of on-axis group- and phase-fringe tracking. We further show that the knowledge to produce science grade data out of such operation is available in the community, and it was used to analyze

the data shown here. Therefore, the authors hope that this article can given some momentum to the efforts of making this promising observing mode accessible to scientific observations.

ACKNOWLEDGMENTS

REFERENCES

[1] Leinert, C., Graser, U., Przygodda, F., Waters, L. B. F. M., Perrin, G., Jaffe, W., Lopez, B., Bakker, E. J., Böhm, A., Chesneau, O., Cotton, W. D., Damstra, S., de Jong, J., Glazenborg-Kluttig, A. W., Grimm, B., Hanenburg, H., Laun, W., Lenzen, R., Ligori, S., Mathar, R. J., Meisner, J., Morel, S., Morr, W., Neumann, U., Pel, J., Schuller, P., Rohloff, R., Stecklum, B., Storz, C., von der Lühe, O., and Wagner, K., "MIDI - the 10 μm instrument on the VLTI," *AP&SS* **286**, 73–83 (2003).

[2] Quirrenbach, A., Coudé du Foresto, V., Daigne, G., Hofmann, K. H., Hofmann, R., Lattanzi, M., Osterbart, R., Le Poole, R. S., Queloz, D., and Vakili, F., "PRIMA: study for a dual-beam instrument for the VLT Interferometer," in [*Astronomical Interferometry*], R. D. Reasenberg, ed., *Proc. SPIE* **3350**, 807–817 (1998).

[3] Delplancke, F., Derie, F., Lévêque, S., Ménardi, S., Abuter, R., Andolfato, L., Ballester, P., de Jong, J., Di Lieto, N., Duhoux, P., Frahm, R., Gitton, P., Glindemann, A., Palsa, R., Puech, F., Sahlmann, J., Schuhler, N., Duc, T. P., Valat, B., and Wallander, A., "PRIMA for the VLTI: a status report," in [*Advances in Stellar Interferometry*], *Proc. SPIE* **6268**, 27–+ (2006).

[4] Schmid, C., Abuter, R., Menardi, S., Andolfato, L., Delplancke, F., Derie, F., Di Lieto, N., Frahm, R., Gitton, P., Gomes, N., Haguenauer, P., Leveque, S., Morel, S., Müller, A., Phan Duc, T., Pozna, E., Sahlmann, J., Schuhler, N., and van Belle, G., "Status of PRIMA for the VLTI or the quest for user-friendly fringe tracking," in [*These Proceedings*], (2010).

[5] Sahlmann, J., Ménardi, S., Abuter, R., Accardo, M., Mottini, S., and Delplancke, F., "The PRIMA fringe sensor unit," *A&A* **507**, 1739–1757 (2009).

[6] Sahlmann, J., Abuter, R., Ménardi, S., Schmid, C., Di Lieto, N., Delplancke, F., Frahm, R., Gitton, P., Gomes, N., Haguenauer, P., Lévêque, S., Morel, S., Müller, A., Phan Duc, T., Schuhler, N., and van Belle, G., "First results from fringe tracking with the PRIMA fringe sensor unit," in [*These Proceedings*], (2010).

[7] Le Bouquin, J., Abuter, R., Bauvir, B., Bonnet, H., Haguenauer, P., di Lieto, N., Menardi, S., Morel, S., Rantakyrö, F., Schoeller, M., Wallander, A., and Wehner, S., "Fringe tracking at VLTI: status report," in [*Optical and Infrared Interferometry*], *Proc. SPIE* **7013** (2008).

[8] Gitton, P. B., Leveque, S. A., Avila, G., and Phan Duc, T., "IRIS: an infrared tilt sensor for the VLTI," in [*New Frontiers in Stellar Interferometry*], W. A. Traub, ed., *Proc. SPIE* **5491**, 944–+ (2004).

[9] Hippler, S., Jaffe, W., Mathar, R., Storz, C., Wagner, K., Cotton, W. D., Perrin, G., and Feldt, M., "MIDI: controlling a two 8-m telescope Michelson interferometer for the thermal infrared," in [*Interferometry in Optical Astronomy*], P. Léna & A. Quirrenbach, ed., *Proc. SPIE* **4006**, 92–98 (2000).

[10] Jaffe, W. J., "Coherent fringe tracking and visibility estimation for MIDI," in [*New Frontiers in Stellar Interferometry*], W. A. Traub, ed., *Proc. SPIE* **5491**, 715–+ (2004).

[11] Beichman, C. A., Neugebauer, G., Habing, H. J., Clegg, P. E., and Chester, T. J., eds., [*Infrared astronomical satellite (IRAS) catalogs and atlases. Volume 1: Explanatory supplement*], **1** (1988).

[12] Tristram, K. R. W., *Mid-infrared interferometry of nearby Active Galactic Nuclei*, PhD thesis, Max-Planck-Institut für Astronomie, Königstuhl 17, 69117 Heidelberg, Germany (2007).

[13] Tristram, K. R. W., Meisenheimer, K., Jaffe, W., Schartmann, M., Rix, H., Leinert, C., Morel, S., Wittkowski, M., Röttgering, H., Perrin, G., Lopez, B., Raban, D., Cotton, W. D., Graser, U., Paresce, F., and Henning, T., "Resolving the complex structure of the dust torus in the active nucleus of the Circinus galaxy," *A&A* **474**, 837–850 (2007).

[14] Fedele, D., van den Ancker, M. E., Acke, B., van der Plas, G., van Boekel, R., Wittkowski, M., Henning, T., Bouwman, J., Meeus, G., and Rafanelli, P., "The structure of the protoplanetary disk surrounding three young intermediate mass stars. II. Spatially resolved dust and gas distribution," *A&A* **491**, 809–820 (2008).

[15] Verhoeff, A. P., Waters, L. B. F. M., Veerman, H., Pantin, E., Min, M., Pel, J. W., Tielens, A. G. G. M., van den Ancker, M. E., van Boekel, R., Boersma, C., Bouwman, J., Dominik, C., de Koter, A., Lagage, P.-O., and Peletier, R. F., "VISIR spectroscopic and spatial survey of Herbig Ae stars," *submitted to A&A* (2010).

[16] Raban, D., Jaffe, W., Röttgering, H., Meisenheimer, K., and Tristram, K. R. W., "Resolving the obscuring torus in NGC 1068 with the power of infrared interferometry: revealing the inner funnel of dust," *MNRAS* **394**, 1325–1337 (2009).

[17] Burtscher, L., Meisenheimer, K., Jaffe, W., Tristram, K. R. W., and Röttgering, H. J. A., "Resolving the nucleus of Centaurus A at mid-IR wavelengths," *submitted to PASA* (2010).

[18] Pott, J., Eckart, A., Glindemann, A., Kraus, S., Schödel, R., Ghez, A. M., Woillez, J., and Weigelt, G., "First VLTI infrared spectro-interferometry on GCIRS 7. Characterizing the prime reference source for Galactic center observations at highest angular resolution," *A&A* **487**, 413–418 (2008).

[19] Segransan, D., Beuzit, J., Delfosse, X., Forveille, T., Mayor, M., Perrier-Bellet, C., and Allard, F., "How AMBER will contribute to the search for brown dwarfs and extrasolar giant planets," in [*Interferometry in Optical Astronomy*], P. Léna & A. Quirrenbach, ed., *Proc. SPIE* **4006**, 269–276 (2000).

[20] Lopez, B., Petrov, R. G., and Vannier, M., "Direct detection of hot extrasolar planets with the VLTI using differential interferometry," in [*Interferometry in Optical Astronomy*], P. Léna & A. Quirrenbach, ed., *Proc. SPIE* **4006**, 407–411 (2000).

[21] Vasisht, G. and Colavita, M. M., "Differential phase interferometry with the Keck telescopes," in [*New Frontiers in Stellar Interferometry*], W. A. Traub, ed., *Proc. SPIE* **5491**, 567–+ (2004).

[22] Vannier, M., Petrov, R. G., Lopez, B., and Millour, F., "Colour-differential interferometry for the observation of extrasolar planets," *MNRAS* **367**, 825–837 (2006).

[23] Queloz, D., Mayor, M., Weber, L., Blécha, A., Burnet, M., Confino, B., Naef, D., Pepe, F., Santos, N., and Udry, S., "The CORALIE survey for southern extra-solar planets. I. A planet orbiting the star Gliese 86," *A&A* **354**, 99–102 (2000).

[24] Vannier, M., *Interférométrie et astrométrie différentielles chromatiques et observation de planètes extra-solaires géantes chaudes avec le VLTI et le NGST*, PhD thesis, Laboratoire Universitaire d'Astrophysique de Nice/Université de Nice-Sophia Antipolis (2003).

[25] Meisner, J. A. and Le Poole, R. S., "Dispersion affecting the VLTI and 10 micron interferometry using MIDI," in [*Interferometry for Optical Astronomy II*], Traub, W. A., ed., *Proc. SPIE* **4838**, 609–624 (2003).

[26] Colavita, M. M., Swain, M. R., Akeson, R. L., Koresko, C. D., and Hill, R. J., "Effects of Atmospheric Water Vapor on Infrared Interferometry," *PASP* **116**, 876–885 (2004).

[27] Meisner, J. A., Tubbs, R. N., and Jaffe, W. J., "Coherent integration of complex fringe visibility employing dispersion tracking," in [*New Frontiers in Stellar Interferometry*], Traub, W. A., ed., *Proc. SPIE* **5491**, 725–+ (2004).

[28] Matter, A., Vannier, M., Morel, S., Lopez, B., Jaffe, W., Lagarde, S., Petrov, R. G., and Leinert, C., "First step to detect an extrasolar planet using simultaneous observations with the VLTI instruments AMBER and MIDI," *accepted by A&A* (2010).